Journal of Wasit for Science and Medicine 2024: 17, (3), 51-65

Evaluation of Gamma Ray Attenuation Properties of Gypsum-wood Ash Composite by Incorporating Micro-Fe Particles

Rafal Kamel Khalaf, and Mohammed Jbur Risn

Department of Physics, College of Science, Wasit University, Wasit, Iraq.

Abstract

NaI (Tl) detector system and Co-60 radioactive isotope were used to study the possibility of improving the radiation attenuation properties of different samples of gypsum-wood ash composite shield reinforced with micro-Fe particles. Seven types of composite shields were prepared, distributed between one sample of gypsum and two of gypsum-wood ash with concentrations of (0.6: 0.4) wt and (0.4: 0.6) wt of gypsum to wood ash respectively. Four samples of gypsum-wood ash-Fe with weight fraction (wt) of 0.36: 0.24: 0.4, 0.24: 0.16: 0.6, 0.24: 0.36: 0.4, and 0.16: 0.24: 0.6, respectively. The values of T %, LAC, MAC, MFP, HVL, RPE%, and dPb were obtained experimentally. These results were then strengthened by conducting a theoretical study of these parameters using the Phy-x/PSD platform and the NGCal program. The results showed that the radiation attenuation properties of gypsum improved significantly when the gypsum-wood ash samples were reinforced with micro-Fe particles, as the 0.6 wt of Fe addition ratio, for GA1F2 and GA2F samples, achieved a significant improvement in the radiation attenuation properties against the gamma rays. The GA1F2 sample recorded the best LAC values of 0.1257 cm^{-1} and 0.1121cm^{-1}, with an increase rate of 70.5563 % and 61.9942 % relative to the gypsum sample (G) for gamma energies of 1.173MeV and 1.333 MeV. The improvement in LAC values was reflected in the values of other parameters, as the GA1F2 composite shield achieved the smallest values of T %, MFP, and HVL and the highest values of MAC, RPE % and dPb. The results of the current study showed that the GA1F2 sample could be suitable for radiation applications and reduce radiation exposure.

Keywords: Shielding, Gamma Attenuation, and Gypsum.

1. Introduction

A high number of people are constantly exposed to radiation emitted from natural sources. In addition to artificial sources resulting from the widespread uses of radiation in various fields such as industry,

agriculture, nuclear reactors, space, and nuclear and radiation medicine [1-3].

Increased exposure to various nuclear radiations exposes great risks to various living organisms. It is necessary to develop appropriate methods and mechanisms to protect people from the harmful effects of these radiations. One of the most important ways to reduce exposure and reduce the impact of radiation is to use protective shields to block the rays or reduce their intensity.

Choosing the appropriate type and thickness of shielding material depends on the type and energy of radiation [4-6]. Various materials were proposed and studied as radiation shields, such as lead, alloys, clay, and concrete. Many researchers referred them as effective alternatives to mitigate the harmful effects of radiation for many reasons, such as high density, cheap price, availability, capacity, and ease of formation [4-7].

Researchers considered the possibility of incorporating building materials as a viable option for radiation protection due to their ease of processing and the availability of their components. One of these alternatives is gypsum, which is considered an essential raw material and is abundantly available, in addition to many other positive qualities [8, 9].

Recently, there has been a trend towards the use of composite materials for radiation protection applications.

These composites combine different materials to enhance shielding properties, allowing the design of shields tailored to specific radiation sources and environments. Moreover, by incorporating these elements and compounds into a matrix material, composite shields can achieve good blocking and attenuation of ionizing radiation [10-12]. There is an increasing demand for the development of new environmentally friendly binders as they play an important role in the overall performance of construction.

Mortar is a composite material that binds building units together and is also useful for distributing the load uniformly on the underlying brick or stone. Gypsum is a synthetic building material used to bond building units, in building ceilings and in interior wall coatings. Moreover, it is used in the medical field as a shield against low-energy X-rays in diagnostic radiology [6].

Theoretical calculations of the mass attenuation coefficients of cement, gypsum, and a mixture of gypsum and $PbCO_3$ were performed using the MCNPX code [7]. In another study, fly ash-lime-gypsum (FaLG) bricks were prepared and the parameters of the accumulation of exposure to energy and dose were studied [13].

The use of many and varied composites based on gypsum as a matrix material has been studied and their radiation attenuation properties have been determined for their possible use in nuclear applications.

The efficiency of radiation shielding against gamma rays has been tested for composites of Gypsum / poly (methyl acrylate) [14]. Gypsum-graphene, and Bi_2O_3 / bentonite–gypsum which showed improved radiation attenuation properties of gypsum [15, 16].

An experimental and theoretical study was conducted using the XCOM database of gamma rays attenuation coefficients for some types of gypsum concrete reinforced with different percentages of boron at different gamma ray's energies showed that increasing the percentage of boron added to gypsum concrete increases the values of the attenuation coefficients and improves the shielding properties of the samples [17].

The efficiency of shield made of gypsum-marble mortars reinforced with different concentrations of micro and nano-powders of PbO was also tested. The experimental results, as well as the theoretical results using the XCOM database for that study, showed that increasing the concentration of PbO in the composite led to an increase in the values of the linear attenuation coefficient (LAC and decrease the half layer thickness (HVL), and the rate of free path (MFP) thus improving the shielding efficiency of the gypsum [18].

In the current study, gypsum is used as a low-cost shielding material, to increase the attenuation efficiency of the composite. Gypsum was reinforced with different proportions of local industrial waste from wood ash with a granularity of up to 50µm and iron powder with a granularity of up to 100µm.

The experimental study was conducted using the NaI(Tl) detector and the Co-60 isotope that emits gamma rays with energies of 1.173 MeV and 1.333 MeV. The experimental study was also supported by two theoretical studies using the Phy-x/PSD platform, and NGCal internet computer program [19, 20].

2. Materials and Methods

2.1 Materials and Samples Preparation

Seven different samples of gypsum, wood ash, and micro-iron particles mixture were prepared. These samples were distributed between one sample of gypsum, two of gypsum and wood ash with different weight fractions.

Other four with different weight fractions of gypsum, wood ash, and micro-Fe particles, as shown in (table 1), clarifies the densities of the prepared samples calculated experimentally and theoretically.

NaI(Tl) scintillation detector system was used, and a narrow beam of gamma rays emitted by the radioactive isotope Co-60. That emits energies of 1.173 and 1.333 MeV gamma rays and obtained using lead collimators with central holes of 0.5 and 1cm for both the source and detector collimators, as shown in (figure 1).

Table 1: Symbols, components, and experimental and theoretical densities of composite shied samples.

Sample code	Contents ratios	Density (g/cm^3)		Error ratio (%)
		Theo.	Expt.	
G	Gypsum	1.2	1.2472	3.9294
GA1	0.6 Gypsum + 0.4 Wood Ash	0.9744	0.9111	6.4971
GA2	0.4 Gypsum + 0.6 Wood Ash	0.8906	0.8995	0.9977
GA1F1	0.6 (0.6 Gypsum + 0.4 Wood Ash) + 0.4 Fe	1.5002	1.5724	4.8118
GA1F2	0.4 (0.6 Gypsum + 0.4 Wood Ash) + 0.6 Fe	2.0546	1.9324	5.9479
GA2F1	0.6 (0.4 Gypsum + 0.6 Wood Ash) + 0.4 Fe	1.3803	1.3372	3.1212
GA2F2	0.4 (0.4 Gypsum + Wood 0.6Ash) + 0.6 Fe	1.9036	1.8334	3.6886

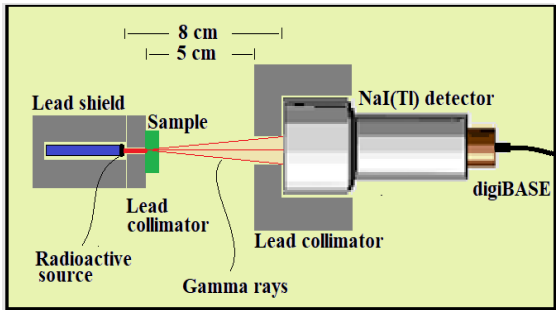

Figure 1: A schematic diagram of the work system.

Samples preparation included local gypsum manufactured in Iraq from Al-Myzan gypsum company, in addition to wood ash from local waste. That which was sieved with a fine sieve with holes measuring 50 µm. Iron powder from local industrial waste was also used, with a particle size of up to 100 µm that was obtained using a sieve of this scale. All shield samples were prepared in a cylindrical shape with a diameter of 1 cm and different thicknesses of 1, 2, and 3 cm. Furthermore, (figure 2) shows shape of the prepared samples used for the current study.

Components of materials used that were used to prepare shield samples and their theoretical densities are also listed in (table 2), which were used to calculate shield densities and perform theoretical calculations intended for this work [19-21]. Enhancing the current experimental study of the prepared samples, two theoretical studies were conducted using the Phy-x/PDS platform, and NGCal computer program [22, 23]. Studies were utilised to calculate radiation attenuation parameters for gamma rays at energies and materials specified by the user.

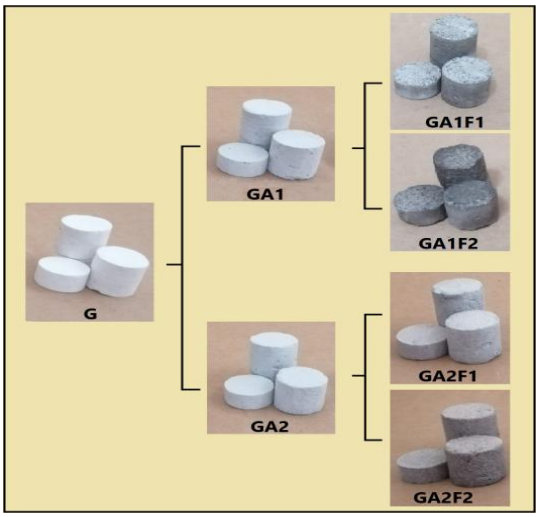

Figure 2: Prepared samples.

Table 2: Chemical formulas and densities of materials used to prepare composite samples.

Material	Chemical formula	Density (g/cm^3)
Gypsum [19]	$CaSO_4.2H_2O$, or (CaH_4SO_6)	1.2
Wood Ash [20]	0.55 SiO_2 + 0.259 Al_2O_3 + 0.074 Fe_2O_3 + 0.057 CaO + 0.02 MgO + 0.02 K_2O + 0.01 SO_3 + 0.01 Na_2O	0.76
Iron [21]	Fe	7.874

2.2 Radiation Measurements

When a parallel beam of gamma rays falls on the material, the incident photon interacts with one of the atoms of the material by any of the three processes. Either because of the absorption of its full energy and its annihilation (by the processes of the photoelectric effect or pair production) or because of its deviation from its path (Compton's phenomenon). Accordingly, the exponential attenuation equation becomes in the form the following [24, 25].

$$I = I_o e^{-\mu x} \quad (1)$$

where I_o, I, and μ represent the incident intensity of gamma rays, the intensity of the rays that penetrate a thickness of material x, and linear attenuation coefficient (LAC). Equation (1) is valid if the photon beam is parallel, narrow and single-energy and the thickness of the absorbing material is very small. It is called the Beer-Lambert equation. This exponential relationship shows that there is no specific range for gamma rays within the material. The relationship (1) can be used to calculate the linear attenuation coefficient as follows

$$Ln\frac{I_o}{I} = \mu x \quad (2)$$

The value of the mass attenuation coefficient (MAC or μm) can be calculated from the value of the LAC according to the following relationship [25].

$$\mu_m = \mu / \rho \quad (3)$$

where ρ represents the density of the substance. If the substance is composed of several elements as a compound, the density of the compound is calculated using the law of mixtures and according to the following equation: [26]

$$\rho_c = \rho_r V_r + (1\text{-}V_r) \rho_m \quad (4)$$

where ρ_c, ρ_r, ρ_m, and V_r represent the density of the composite material, the density of the reinforcement material, the density of the matrix material, and the volume fraction used for the reinforcement material. The volume fraction is calculated from the following relationship

$$V_r = \frac{\frac{W_r}{\rho_r}\%}{\frac{W_r}{\rho_r}\% + \frac{W_m}{\rho_m}\%} \quad (5)$$

where W_r represents the weight fraction of the reinforcement material, and W_m represents the weight fraction of the matrix material. Recently, researchers have focused on studying the parameters of the interaction of photons with various materials, such as (attenuation coefficient, transmittance, half-layer thickness, free

path rate, radiation protection efficiency, etc.). Due to the frequent use of radioactive sources in various fields such as the industrial field, the medical field, and others. The total attenuation coefficient (linear or mass) depends on the cross section of each of the three main reactions in attenuation.

These cross sections depend on both the energy of the interacting photons and the atomic number of the medium with which they interact, and vary according to the energy and atomic number, where the photoelectric attenuation coefficient (μph) is dominate in low-energy photons and materials with high atomic numbers.

The attenuation coefficient of the Compton effect (μco) is dominate in materials with medium photon energy and low atomic number, and at high photon energy and in materials containing a large number of atoms, the pair production attenuation coefficient (μpp) dominates [27]. The path length that the gamma rays beam travels inside the target material before removing it from the radiation beam, which is called the Mean Free Path (MFP), can be found as the following relationship [24, 28].

$$MFP = \frac{1}{\mu} \quad (6)$$

The concept of the half value layer (HVL) of a material is the thickness required to reduce the intensity of the rays falling on the material to half its value, and it can be calculated by the following equation [28, 29].

$$HVL = \frac{ln\,2}{\mu} \quad (7)$$

The permeability of a material to rays, or what is called the Transmission Factor (T) in any material, can be determined through the following relationship [24, 25, 30].

$$T = \frac{I}{I_0} = e^{-\mu x} \quad (8)$$

Another parameter can also be determined in the subject of radiation shielding, which is Radiation Protection Efficiency (RPE). That represents an important parameter to indicate the efficiency of the shield in protecting against radiation and can be calculated from the following equation [31, 32].

$$RPE = (1- e^{-\mu x}) \times 100\% \quad (9)$$

The thickness of Pb needed to achieve the same effect of shielding against gamma radiation is called the lead equivalent thickness (dPb) and given as [33].

$$d_{Pb} = d_{shield} \times \frac{\mu_{shield}}{\mu_{Pb}} \quad (10)$$

Where μ_{Pb} represents the linear attenuation coefficients of lead and μ_{shield} represents the linear attenuation coefficients of shielding material of thickness d_{shield}.

3. Results and Discussion

Experimental measurements of the change in intensity values of incident gamma rays and penetrating through shield samples emitted from a C0-60 source obtained from a scintillation detector system for a counting time of 1800 seconds, and the resulting values of the gamma ray intensities and the natural logarithm of the count rate ratios are listed in (table 3).

The percentage of transmittance of rays can be studied directly from the values of the intensity of the incident and transmitted gamma rays using equation (8), by plotting the values of the percentage of transmittance (T %) as a function of the thickness and type of the shield, as shown in (figure 3).

From (figure 3) showed that the T% values at any ray energy are the largest possible for the GA1 shield, while their values are the smallest possible for the GA1F2 shield and for all corresponding thickness values. This behaviour is consistent with the results of previous studies [34-36].

Table 3: Values of the gamma ray intensities (I) and the Ln (I_o/I) as a function of gamma energy and shield sample thickness.

Shield code	X (cm)	E = 1.173 MeV				E = 1.333 MeV			
		I (cont/1800s)			Ln $(I_o/I)_{ave.}$	I (cont/1800s)			Ln $(I_o/I)_{ave.}$
		I_1	I_2	$I_{ave.}$		I_1	I_2	$I_{ave.}$	
Non	0	39027	41315	40171	0	37787	35258	36522.5	0
G	1	37325	36656	36990.5	0.068587	33648	34555	34101.5	0.068587
	2	33724	34524	34124	0.141107	32427	31005	31716	0.141107
	3	33204	32066	32635	0.205772	29138	30322	29730	0.205772
GA1	1	38626	37170	37898	0.043452	35037	34902	34969.5	0.043452
	2	34963	36180	35571.5	0.110645	32297	33097	32697	0.110645
	3	34327	33101	33714	0.169165	31105	30572	30838.5	0.169165
GA2	1	37458	38840	38149	0.042423	35098	34913	35005.5	0.042423
	2	36109	35374	35741.5	0.095785	32904	33469	33186.5	0.095785
	3	33916	34480	34198	0.156806	31313	31131	31222	0.156806
GA1F1	1	35824	34924	35374	0.109927	32326	33115	32720.5	0.109927
	2	32426	34291	33358.5	0.178187	31772	29351	30561.5	0.178187
	3	31025	30523	30774	0.245606	28663	28475	28569	0.245606
GA1F2	1	33651	34088	33869.5	0.159821	30816	31440	31128	0.159821
	2	31145	30877	31011	0.233049	29463	28397	28930	0.233049
	3	28478	27725	28101.5	0.31452	27261	26072	26666.5	0.31452
GA2F1	1	36413	35961	36187	0.095921	33410	32954	33182	0.095921
	2	32824	33935	33379.5	0.143491	32088	31193	31640.5	0.143491
	3	31401	32015	31708	0.237362	28509	29102	28805.5	0.237362
GA2F2	1	33924	34742	34333	0.137802	31542	32100	31821	0.137802
	2	32328	31224	31776	0.21061	28901	30272	29586.5	0.21061
	3	29982	28725	29353.5	0.305319	27425	26401	26913	0.305319

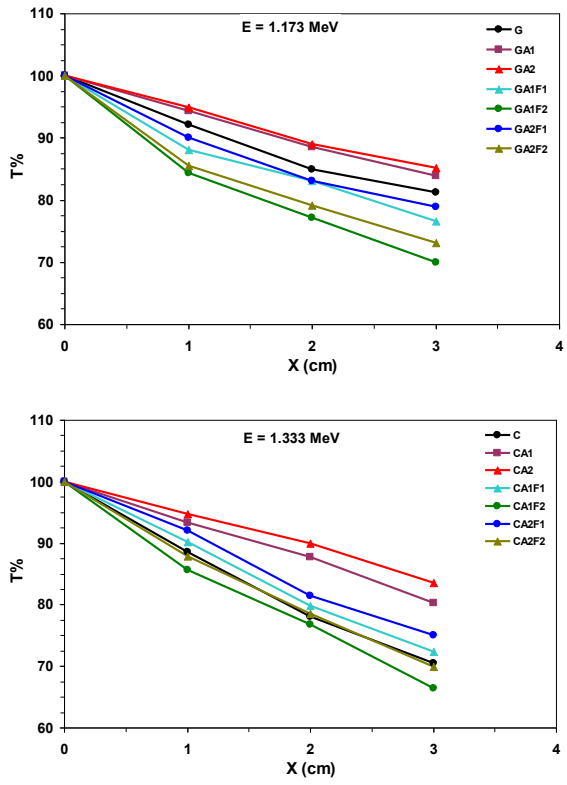

Figure 3: Variation T % values as a function of thickness shield samples (x) for all shield samples at 1.173 MeV, and 1.333 MeV gamma ray energy.

Plotting the linear relationship for the values of Ln (Io/I) as a function of the thickness of the shield material gives the values of the linear attenuation coefficients (LAC) according to equation (2). For this purpose, that relationship was shown in (figure 4) at the energies 1.173, and 1.333 MeV.

From the equations of the linear relationships shown in the figure which showed a great match with the drawn data where the R2 values showed a great match, as their values were within the range 0.9473-0.9995. LAC values can be obtained for all shield samples studied, which represent the slope of the relationship line.

Moreover, (table 4) shows values of the linear attenuation coefficients (LAC) calculated from the linear relationships in (figure 4) and plotted as a function of gamma ray energy and the type of shield used in (figure 5). The increment (Δ%) between the experimental values and the Phy-x/PSD and NGCal theoretical values of LAC were calculated using the following equation [24].

$$\Delta\% = \frac{\mu_{expt.} - \mu_{theo.}}{\mu_{theo.}} \quad (11)$$

This parameter shows the increase achieved in the LAC values in the prepared shields relative to their values in the gypsum sample (G). Results of (table 4) showed that an increase was achieved in the LAC values for shields of GA2F1, GA1F1, GA2F2, and GA1F2, and the largest increase recorded was for sample GA1F2, where it reached 70.5563 % and 61.9942 % at energies of 1.173 MeV and 1.333 MeV respectively.

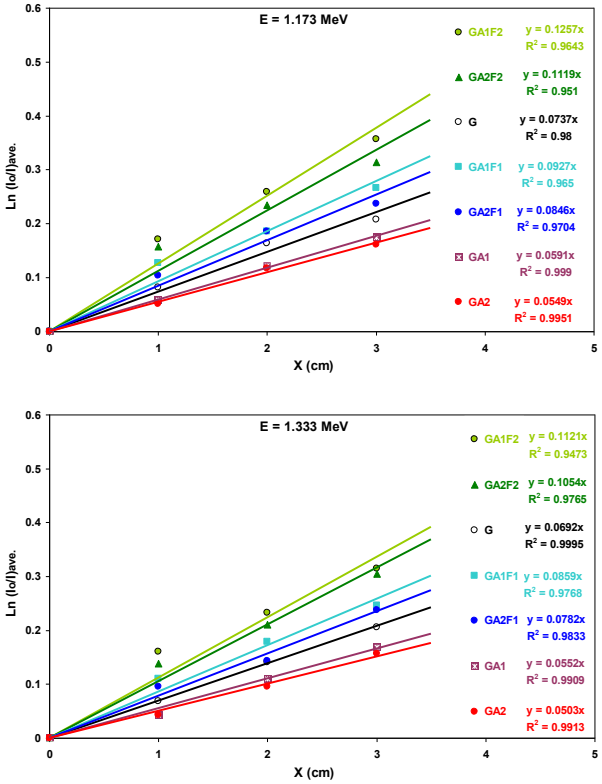

Figure 4: Values of Ln (Io/I) as a function of thickness shield samples (x) for all shield samples at 1.173 MeV and 1.333 MeV gamma ray energy.

Table 4: Values of LAC and Δ% as a function of gamma energy for all shield sample.

Shield code	E = 1.173 MeV		E = 1.333 MeV	
	LAC (cm^{-1})	Δ%	LAC (cm^{-1})	Δ%
G	0.0737	0	0.0692	0
GA1	0.0591	-19.8100	0.0552	-20.2312
GA1F1	0.0927	25.7802	0.0859	24.1330
GA1F2	0.1257	70.5563	0.1121	61.9942
GA2	0.0549	-25.5088	0.0503	-27.3121
GA2F1	0.0846	14.7897	0.0782	13.0058
GA2F2	0.1119	51.8318	0.1054	52.3121

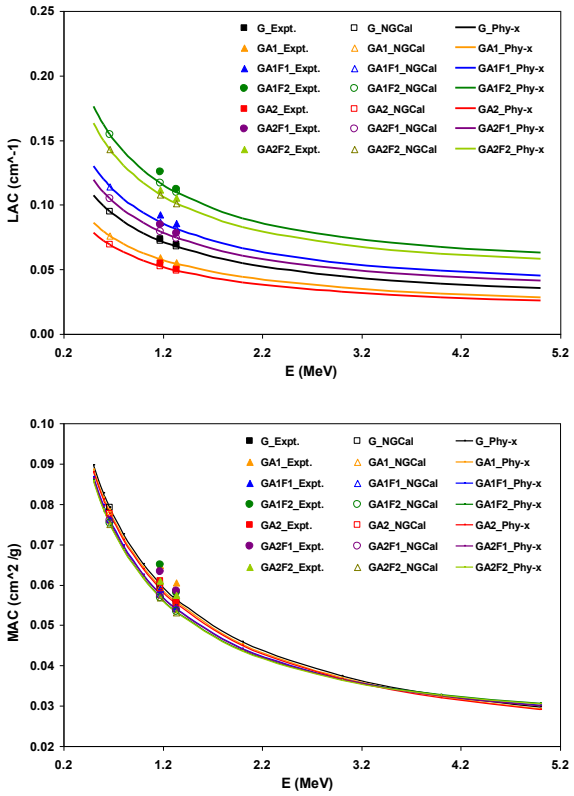

Figure 5: Variation of LAC and MAC as a function of gamma ray energy for all shield samples.

Variation of the experimental and theoretical LAC and mass attenuation coefficients (MAC) values are displayed in (figure 5). Calculation using equation (3) for experimental shield samples densities as well as the theoretical values for the calculations of the Phy-x/PSD platform and NGCal program as a function of gamma rays and for all shield samples. From (figure 4) Values of the LAC and MAC decrease with increasing gamma ray energy for all prepared shield samples.

The reason for this is that increasing energy reduces the probability of the occurrence of the photoelectric effect interaction, which prevails at low energies. As Compton scattering interaction effect begins to appear in the medium energies range and then values of these coefficients begin to decrease in a less steep manner after energy 1.173 MeV due to the appearance of the interaction contribution of pair production occurs at energies greater than 1.22 MeV [37].

This is consistent with the results of previous studies where experimental and theoretical values showed a great match for LAC, and MAC [37, 38]. Study variations of MFP and HVL values for the prepared samples, equations (6) and (7) were used. The experimental, and theoretical results were plotted as a function of shield type and gamma ray energy in (figure 6).

From (figure 6) MFP increases with increasing gamma ray energy for all shield samples, and values of this parameter are largest possible for the GA2 sample and the smallest possible for the GA1F2 sample. For values of studied energies, we found that values of the parameter increased from 13.5685 cm to 14.4509 cm for the G sample.

Moreover, from 7.9555 cm to 8.9206 cm for the GA1F2 sample when gamma ray's energies values change from 1.173 MeV to 1.333 MeV. It is also noted that, HVL values increase with the increase in gamma ray energy for all prepared shield samples. That behaviour of change in the

HVL values is like the behaviour of the MFP values with the gamma ray energy. As opposite to the behaviour of μ also due to the inverse relationship between them. The behaviour is consistent with previous studies based on the calculation results [39, 40].

Also, HVL values increased from 9.4049 cm to 10.01658 cm for the G sample, as well as from 5.5143 cm to 6.1833 cm for GA1F2 sample when the gamma ray's energies values changed from 1.173 MeV to 1.333 MeV, respectively. GA1F2 sample achieved the best results among the prepared samples for both energies. In addition, the experimental values of MFP and HVL achieved a close match with theoretical values [40-42].

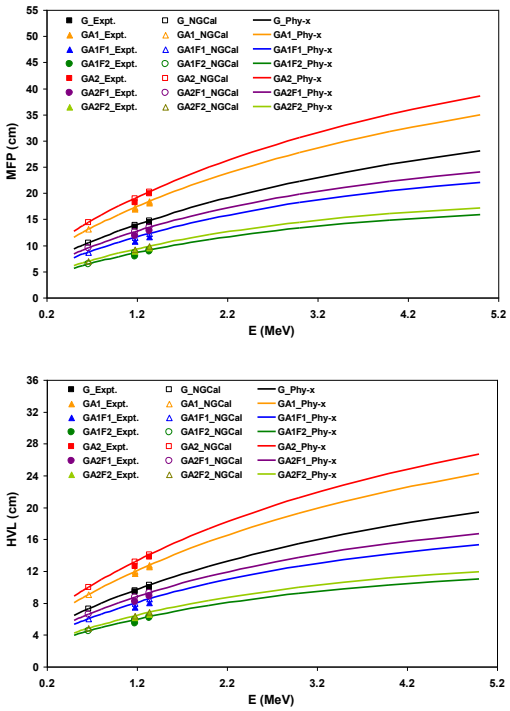

Figure 6: Variation of MFP and HVL as a function of gamma ray energy for all shield samples.

An adequate description to the efficiency of prepared shield samples for radiation uses the radiation protection efficiency (RPE) parameter. This parameter was studied using equation (9).

The experimentally and theoretically percentages of the radiation protection efficiency (RPE %) values at 1 cm sample thickness for all the prepared shield samples were plotted as a function of gamma ray's energies in (figure 7).

From (figure 7) RPE % values at any of the two gamma rays energies are smallest possible for the GA1 shield, while their values are the largest possible for the GA1F2 shield and for all corresponding thickness values.

The highest values of RPE % were achieved at 3 cm thickness for the induced sample GA1F2 where its values were 31.4153 % and 28.5591 % at energies 1.173 MeV and 1.333 MeV correspondingly. Increasing shield thickness improves significantly, and this behaviour is consistent with the results of previous studies [34, 36].

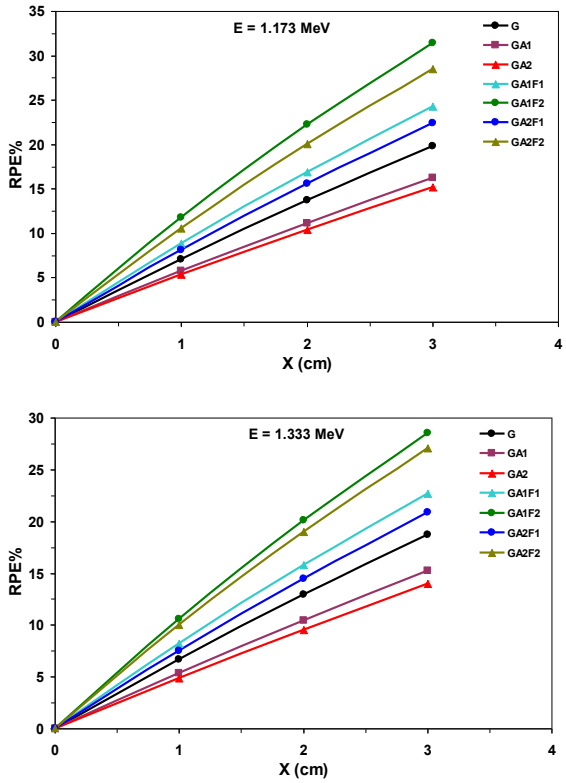

Figure 7: Variation RPE % values as a function of thickness shield samples (x) for all shield sample at 1.173 MeV and 1.333 MeV gamma ray energy.

Lead equivalent thickness (dPb) that represent the thickness of Pb needed to achieve the same effect of shielding against gamma radiation was calculated by equation (10). However, (figure 8) shows changes in lead equivalent thickness values for prepared shield samples, by variation type and thickness of shield for each of the gamma ray energies studied. The last figure shows that the dPb in the gypsum sample began to increase and improve in samples of GA2F2, and GA1F2, separately.

This parameter achieved the best value using sample GA1F2 and for both gamma ray energies.

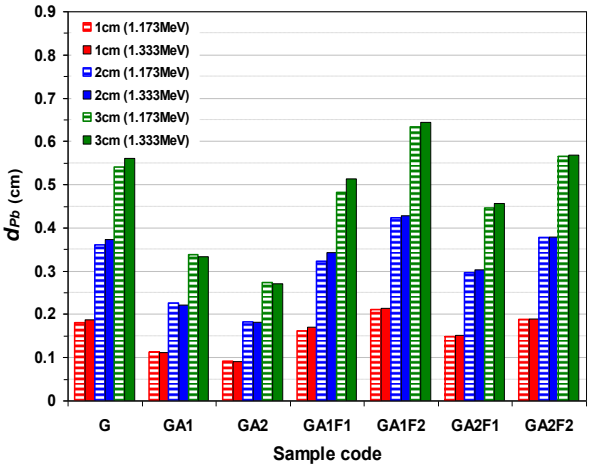

Figure 8. Values of dPb as a function shield sample type.

4. Conclusion

Studying the preparation of radiation shields from available, low-cost materials, and industrial waste is very important for achieving sustainable development and waste recycling. Results of the radiation tests conducted experimentally and theoretically in the current study showed that the radiation attenuation properties of gypsum can be improved by adding wood ash and iron waste. Values of radiation attenuation parameters improved by increasing reinforcement of gypsum-wood ash samples with micro-Fe particles. The radiation attenuation properties improved greatly in the GA1F2 and GA2F2 shields, and values of RPE %, and dPb were the highest possible. Values of MFP, HVL, and T % were lowest possible using GA1F2 shield sample. The results of the study also showed that as gamma ray energy

increases, the values of LAC, MAC, and RPE % decrease while the values of MFP, HVL, and dPb increase. In addition, increasing the thickness of the shield material, led to a decrease in T % values and an increase in RPE % values. Finally, shields of GA1F2, and GA2F2 can be considered as suitable shields for use in some suitable radiation applications.

5. References

1. Kilic G., Issa S., Ilik E., Kilicoglu O., İşsever U., El-Mallawany R., Issa B., and Tekin H., (2021). Physical, thermal, optical, structural and nuclear radiation shielding properties of Sm_2O_3 reinforced borotellurite glasses. Ceramics International. 47. 6154-6168.
2. Hernandez-Murillo C. G., Escalera-Velasco L. A., de Leon-Martínez H. A., Vega-Carrillo H. R., Molina Contreras J. R., Moreira Del Rio D. E., and Jauregui Acevedo D., (2022). Characteristics, as a shield against ionizing photons, of concrete blocks used in the construction industry. Applied radiation and isotopes: including data, instrumentation and methods for use in agriculture, industry and medicine. 187, 110343.
3. Almuqrin A. H., Sayyed M. I., Elsafi M., and Khandaker M. U., (2022). Comparison of radiation shielding ability of Bi_2O_3 micro and nanoparticles for radiation shields. Radiation Physics and Chemistry. 200.
4. Sriwongsa K., Ravangvong, S., Sngthon, K., Kornponggun, B., and Glumglomchit, P., (2021). Coconut Dust Gypsums Board Building Material for Shielding Radiation and Buildup Factors. Walailak Journal of Science and Technology (WJST). 18, 8, 9350.
5. Hamad M. K, Mhareb M. H., Sayyed M. I., Alajerami Y. S., Alsharhan R., and Khandaker M. U., (2022). Novel efficient alloys for ionizing radiation shielding applications: a theoretical investigation. Radiation Physics and Chemistry. 200, 110181.
6. AbuAlRoos N. J., Amin N. A., and Zainon R., (2019). Conventional and new lead-free radiation shielding materials for radiation protection in nuclear medicine: A review. Radiation Physics and Chemistry. 165, 108439.
7. Singh V. P., Badiger N. M., and Kaewkhao J., (2014). Radiation shielding competence of silicate and borate heavy metal oxide glasses: comparative study. Journal of non-crystalline solids. 404, 167-173.
8. Hagiri M., and Honda K., (2021). Preparation and evaluation of gypsum plaster composited with copper smelter slag. Cleaner Engineering and Technology. 2,100084.
9. Jeong S. G., Chang S. J., Wi S., Lee J., and Kim S., (2017). Energy performance

evaluation of heat-storage gypsum board with hybrid SSPCM composite. Journal of Industrial and Engineering Chemistry. 51, 237-243.

10. Magallanes-Rivera R. X., Juarez-Alvarado C. A., Valdez P., and Mendoza-Rangel J. M., Modified gypsum compounds: An ecological-economical choice to improve traditional plasters. Construction and building materials. 37, 591-596.
11. Verma A., and Yadav M., (2021). Application of nanomaterials in architecture-An overview. Materials Today: Proceedings. 43, 2921-2925.
12. Papadaki D., Kiriakidis G., and Tsoutsos T., (2018). Applications of nanotechnology in construction industry. In Fundamentals of nanoparticles. 343-370. Elsevier.
13. Sidhu B. S., Dhaliwal A. S., Kahlon K. S., and Singh S., (2022). On the use of flyash-lime-gypsum (FaLG) bricks in the storage facilities for low level nuclear waste. Nuclear Engineering and Technology. 54, 2, 674-680.
14. Zaki A. J., (2008). Radiation-induced preparation of gypsum/poly (methyl acrylate) composites. Revue Roumaine de Chimie. 53, 11, 1065-1068.
15. Martinez Gordon A., and Prieto Barrio M. I., (2023). Radiation Shielding Competence of Gypsum-Graphene Composites: A Comparative Study. Available at SSRN 4462754.
16. Abbas M. I., El-Khatib A. M., Elsafi M., El-Shimy S. N., Dib M. F., Abdellatif H. M., Baharoon R., and Gouda M. M., (2023). Investigation of Gamma-Ray Shielding Properties of Bismuth Oxide Nanoparticles with a Bentonite-Gypsum Matrix. Materials. 16, 5, 2056.
17. Günoğlu K., (2017). Radiation transmission of some gypsum concretes for 511, 835 and 1275 keV gamma rays. Acta Physica Polonica A.132, 3, 1022-1024.
18. Alabsy M.T., Gouda M. M., Abbas M.I., Al-Balawi S. M., and El-Khatib A. M., (2023). Enhancing the Gamma-Radiation Shielding Properties of Gypsum–Lime–Waste Marble Mortars by Incorporating Micro- and Nano-PbO Particles. Materials. 16, 1577.
19. Avcıoğlu C., and Avcıoğlu S., (2023). Transition Metal Borides for All-in-One Radiation Shielding. Materials (Basel, Switzerland). 16, 19, 6496.
20. Ngaaje N. N., (2021). Physico-mechanical properties of plaster of Paris (Gypsum plaster) reinforced with paper pulp. European Journal of Engineering and Technology Research. 6, 1, 124-132.
21. Abdullahi M., (2006). Characteristics of wood ash/OPC concrete. Leonardo Electronic Journal of Practices and Technologies. 8.

22. John Rumble, (1997). Handbook of Chemistry and Physics, 78th edition, C R C Press, Boca Raton, Florida, 1997.
23. Şakar E., Team, Phy-X & Alım, Bünyamin and Kurudirek M., (2019). Phy-X / PSD: Development of a user friendly online software for calculation of parameters relevant to radiation shielding and dosimetry. Radiation Physics and Chemistry. 166.
24. Tekin H. O., Bilal G., Zakaly H. M. H., Kilic G., Issa S. A. M., Ahmed E. M., Rammah Y. S., and Ene A., (2021). Newly Developed Vanadium-Based Glasses and Their Potential for Nuclear Radiation Shielding Aims: A Monte Carlo Study on Gamma Ray Attenuation Parameters. Materials (Basel, Switzerland). 14, 14, 3897.
25. Gökçe H. S., Güngör O., and Yılmaz H., (2021). An online software to simulate the shielding properties of materials for neutrons and photons: NGCal. Radiation Physics and Chemistry. 185, 109519.
26. Alabsy M. T., Gouda M. M., Abbas M. I., Al-Balawi S. M., and El-Khatib A. M., (2023). Enhancing the gamma-radiation-shielding properties of gypsum–lime–waste marble mortars by incorporating micro-and nano-PbO particles. Materials.16, 4, 1577.
27. Aldhuhaibat M. J., Amana M. S., Haydar Aboud b., and Salim A. A., (2022). Radiation attenuation capacity improvement of various oxides via high density polyethylene composite reinforcement. Ceramics International. 48, 25011–25019.
28. Aldhuhaibat M. J. R., Amana M. S., Jubier N. J., Salim A. A., (2021). Improved gamma radiation shielding traits of epoxy composites: Evaluation of mass attenuation coefficient, effective atomic and electron number. Radiation Physics and Chemistry. 179, 109183.
29. Williams M. L., and Kim K. S., (2012). The embedded self-shielding method. Advances in Reactor Physics – Linking Research, Industry, and Education (PHYSOR). 15-20.
30. Yasser H. K., Aldhuhaibat M. J., and Farhan A. J., (2024). Investigation of mechanical and radiative attenuation traits of PMMA/ZnO/Bi_2O_3 hybrid nanocomposites. In AIP Conference Proceedings. 2922, 1.
31. Aldhuhaibat M. J., Farhan H. S., Hassani R. H., Tuma H. M., Bakhtiar H., and Salim A. A., (2022). Gamma photons attenuation features of PbO-doped borosilicate glasses: a comparative evaluation. Applied Physics A. 128, 12, 1058.
32. Aldhuhaibat M. J., Amana M. S., Aboud H., and Salim A. A., (2022). Radiation attenuation capacity improvement of various oxides via high density polyethylene composite reinforcement.

Ceramics International. 48, 17, 25011-25019.

33. Şakar E., Özpolat F., Alım B., Sayyed M. I., Kurudirek M., (2020). Phy-X / PSD: Development of a user friendly online software for calculation of parameters relevant to radiation shielding and dosimetry. Radiation Physics and Chemistry. 166, 108496.
34. Aldhuhaibat M. J. R., Farhan H. S., Hassani R., Tuma H. M., Bakhtiar H., Salim A. A., (2022). Gamma photons attenuation features of PbO doped borosilicate glasses: a comparative evaluation, Applied Physics A. 128,1058.
35. Aldhuhaibat M. J. R., Amana M. S., Aboud H., and Salim A. A., (2022). Radiation attenuation capacity improvement of various oxides via high density polyethylene composite reinforcement. Ceramics International. 48, 25011-25019.
36. Mehranpour S., (2020). Comparison of beta, neutron and gamma attenuation properties of pmma/colemanite composites. Master's thesis, Enerji Enstitüsü.
37. Críssia F., Neto A., Santos A. and Faria L., (2016). P(VDF-TrFE)/ZrO2 Polymer-Composites for X-ray Shielding. Materials Research. 19. 10.1590/1980-5373-MR-2015-0576.
38. Alhammashi M. A., Alattabi H. D., and Aldhuhaibat M. J., (2020). Improving the attenuation Ability of gamma rays for silicate glass system composites (GS-PbO): a comparative theoretical study. In IOP Conference Series: Materials Science and Engineering. 928, 7, 072077.
39. Hehn G. (1986). Principles of radiation shielding. Nuclear Technology. 74, 1, 104-105.
40. Albarzan B., Hanfi M. Y., Almuqrin A. H., Sayyed M. I., Alsafi H. M., and Mahmoud K. A., (2021). The influence of titanium dioxide on silicate-based glasses: An evaluation of the mechanical and radiation shielding properties. Materials. 14, 12, 3414.
41. Cao D., Yang G., Bourham M., and Moneghan D., (2020). Gamma radiation shielding properties of poly (methyl methacrylate)/Bi_2O_3 composites. Nuclear Engineering and Technology. 52, 11, 2613-2619.
42. Almuqrin A. H., and Sayyed M. I., (2021). Gamma ray shielding properties of Yb^{3+}-doped calcium borotellurite glasses. Applied Sciences. 11, 12, 5697.